thione)$_4^+$, 47421-11-4; Cu(tetrahydro-3,5-dimethyl-4*H*-1,3,5-oxadiazene-4-thione), 58188-39-9; Cu(thiourea)$_4^+$, 36252-51-4; Cu(1-acetylthiourea)$_4^+$, 58188-40-2; Cu(1-allylthiourea)$_4^+$, 58188-41-3; Cu(1,3-diallylthiourea)$_4^+$, 58188-42-4; Cu(1-methylthiourea)$_4^+$, 58188-43-5; Cu(1,3-dimethylthiourea)$_4^+$, 31248-33-6; Cu(1-ethylthiourea)$_4^+$, 58188-44-6; Cu(1,3-diethylthiourea)$_4^+$, 58188-45-7.

References and Notes

(1) R. C. Martin and W. T. Abel, U.S. Patent 2959555 (1960).
(2) J. G. Frost and B. B. Arnold, U.S. Patent 3547697 (1970).
(3) J. A. Knox, J. A. Smith, and R. R. Stout, U.S. Patent 3730901 (1973).
(4) J. E. Allan, *Spectrochim. Acta*, **17**, 459 (1961).
(5) J. P. Engle, *Combustion*, **33** (8), 41 (Aug 1961).
(6) T. Lane, J. V. Quagliano, and E. Bertin, *Anal. Chem.*, **29**, 481 (1957).
(7) E. I. Onstott and H. A. Laitinen, *J. Am. Chem. Soc.*, **72**, 4724 (1950).
(8) A. T. Pilipenko, *Ukr. Khem. Zh.*, **19**, 81 (1953); K. B. Yatsimirskii and V. P. Vasiley, "Instability Constants of Complex Compounds", Consultants Bureau, New York, N.Y., 1960, p 125.
(9) T. Lane, *Adv. Polarogr., Proc. Int. Congr.*, **2**, 797 (1959).
(10) C. F. H. Allen, C. O. Edens, and J. Van Allen, *Org. Synth.*, **26**, 34 (1946).
(11) M. D. Hurwitz and R. W. Auten, U.S. Patent 2613211 (1952).
(12) I. M. Kolthoff and J. J. Lingane, "Polarography", Interscience, New York, N.Y., **1952**, p 214.
(13) D. D. DeFord and D. N. Hume, *J. Am. Chem. Soc.*, **73**, 5321 (1951).
(14) D. J. Lloyd and A. J. Parker, *Tetrahedron Lett.*, 5183 (1968).
(15) R. G. Salomon and J. K. Kochi, *J. Am. Chem. Soc.*, **95**, 1889 (1973).
(16) W. A. Spofford, III, and E. L. Amma, *Chem. Commun.*, 405 (1968).
(17) W. A. Spofford, III, and E. L. Amma, *Acta Crystallogr., Sect. B*, **26**, 1474 (1970).
(18) F. Hanic and E. Durcauska, *Inorg. Chim. Acta*, **3**, 293 (1969).
(19) A. Streitwieser, "Molecular Orbital Theory for Organic Chemists", Wiley, New York, N.Y., 1961, p 36.
(20) R. G. Vranka and E. L. Amma, *J. Am. Chem. Soc.*, **88**, 4270 (1966).

Contribution from the Institute of Inorganic Chemistry, University of Fribourg, CH-1700 Fribourg, Switzerland

Metal Complexes of Free Radicals. IV.[1] Electrolytic Generation, Complex Equilibria, and Electronic Structure

S. RICHTER, C. DAUL, and A. v. ZELEWSKY*

Received July 11, 1975 AIC50480X

The radical–ligand complex Zn(glir)$^+$, where glir$^-$ is the radical anion of glyoxal bis(*N-tert*-butylimine), has been generated by an electrolytic method within the ESR cavity. This species shows further complex formation with other ligands X. In the case of unidentate ligands X (X^- = Cl^-, Br^-, I^-, NCS^-, NCO^-, N_3^-) 1:1 and 1:2 complexes (only 1:1 for I^-) are formed in a stepwise manner. With the bidentate ligand en only a 1:1 complex was observed. A complex with two coordinated diimine ligands which are in a collectively reduced ground state has also been observed. SCCC–MO calculations are in qualitative agreement with the observed ESR parameters.

Introduction

In the previously applied methods[2] for the preparation of radical complexes of the type M(diir)X_n, where diir is the radical anion[3] of an α-diimine ligand, an alkali metal M or the metal M forming the complex was used as the reducing agent. The former is a two-step and the latter a one-step reaction as shown for an example by eq 1 and 2, where gli = glyoxal bis(*N-tert*-butylimine) and glir$^-$ = radical anion of gli.

$$K + gli \rightarrow K^+ + glir^- \quad (1a)$$

$$ZnX_2 + glir^- \rightarrow Zn(glir)X_n + (2-n)X^- \quad (n = 1 \text{ or } 2) \quad (1b)$$

$$Zn + ZnX_2 + 2gli \rightarrow 2Zn(glir)X \quad (2)$$

Because of the extreme sensitivity of the radical complexes the preparations are carried out[2] in an all-glass system sealed after complete degassing on a vacuum line. This method is therefore not suitable for the investigation of concentration-dependent phenomena, because it does not allow a precisely controlled variation of the concentrations.

An electrolytic cell (see Experimental Section) was developed in which radical complexes can be produced in the ESR cavity and which allows at the same time for a controlled change of concentrations of the reactants. The concentration-dependent studies were conducted with the aim of establishing the nature of equilibria involving complexes M(glir)X_n by varying n and using different ligands X. The spin-labeled ligand[4] glir$^-$ serves as a convenient probe for detection of these complexes and also for the spin density distribution, since the magnetic nuclei in the coordinated glir *and* in the ligands X give rise to hyperfine splittings. This provides some of the most direct information available on electron delocalization in complexes of d^{10} or d^0 metal ions and will be correlated with results from semiempirical calculations. Another advantage of the electrolytic method is the possibility of carrying out reductions in solvents with a high dielectric constant, such as dimethylformamide (DMF), with a consequently much higher solubility of the metal compounds compared with the dimethoxyethane (DME) or tetrahydrofuran (THF), which were used for alkali metal reduction.

Experimental Section[1b]

A. Materials. All chemicals, unless indicated below, were of the highest purity obtainable and were used as received.

Dimethylformamide (Fluka puriss), which was used as a general solvent for all the experiments described in this paper, was shaken for 2 h with NaOH pellets and then for 2 h with KH_2PO_4 (dried at 140 °C), filtered, distilled at 80 °C over molecular sieves (Union Carbide 3 Å), and stored in an argon atmosphere over molecular sieves. Before use it was distilled directly from the storage vessel into a container connected to the electrolytic cell.

Argon was purified with BTS-Catalyst (Fluka AG) and then dried over P_2O_5.

$Zn(DMF)_6(ClO_4)_2$ was prepared according to a reported method[5] and analyzed for Zn.

Glyoxal bis(*N-tert*-butylimine) was prepared as described before.[2]

Tetraethylammonium perchlorate (TEAP) was obtained from a solution of tetraethylammonium hydroxide (Fluka) and perchloric acid. It was recrystallized two or three times until it showed no impurity in a polarogram in DMF (10^{-1} M solution).

The anionic ligands Cl^-, Br^-, I^-, NCS^-, and NCO^-, were all introduced in the solution as their tetraethylammonium salts. These were prepared either by neutralization of the hydroxide with the corresponding acids (Cl^-, Br^-, I^-, NCS^-) or by metathetical reactions (exchange of Br^- with AgNCO). Azide ion was introduced as sodium azide.

Ethylenediamine was stored over NaOH and was freshly distilled before use.

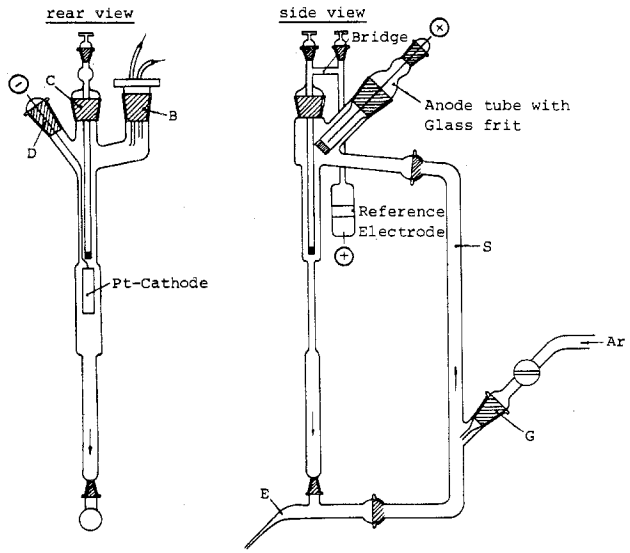

Figure 1. Electrolytic cell used for the generation of radical complexes in the ESR cavity. The reference electrode is immediately above the Pt cathode.

B. Instrumentation and Measuring Procedure. ESR spectra were measured with a Varian E-9 spectrometer equipped with a Varian 620/L computer and interface for instrument control and simulation of spectra.

Electrolyses were carried out in a cell shown in Figure 1. The solution was circulated by bubbles of Ar (~20 bubbles/min) introduced at point G to rise within the tube S. Reduction was carried out at a Pt cathode in the flat part of the quartz cell. As a reference electrode a calomel electrode in DMF was used. It was prepared in exactly the same way as the calomel electrode in acetonitrile described by Bravo et al.[6] but with DMF as a solvent. It showed a constant potential during several months when measured against an aqueous calomel electrode. Reduction was carried out with a three-electrode technique; the voltage was held constant between reference electrode and platinum cathode by a potentiostat (Tacussel PRT 30 0.1). Solutions containing the ligands could be titrated from piston burettes to the cell through Teflon tubes entering at B (Figure 1).

A stock solution containing 10^{-1} M TEAP, 5×10^{-3} M Zn(DMF)$_6$(ClO$_4$)$_2$, and 2.5×10^{-3} M gli in DMF was used for all titrations. In the titrand solutions the concentration of TEAX (or the appropriate reagent) plus TEAP was 10^{-1} M. For most cases two different concentrations of TEAX were chosen. The nonionic ligands en and gli were added to a stock solution (TEAP) and then used for titrations. Electrolysis was started when the cell contained only the stock solution and then the titrand was added in small portions. If necessary known amounts of the solution could be removed with a syringe from the system keeping the total volume within the capacity of the cell. After adding titrand solution, equilibrium was reached in less than 10 min. The ESR spectra reported in this publication were all obtained under very similar conditions: microwave power, 5–10 mW; modulation amplitude, less than half line width; magnetic field range, 10 mT; temperature, ~25 °C; reduction potential, −1.0 to −1.75 V vs. DMF calomel electrode; reduction current, ~0.1 mA.

Results and Interpretation

Identification of Radical Complexes and Equilibrium Data. Electrolysis of the stock solution yields a spectrum as shown in Figure 2. Its main features are the seven lines (1:4:8:10:8...) which we interpret as being due to Zn(glir)$^+$ with an accidental degeneracy of the coupling constants a_H and a_N in the coordinated glir. This behavior has already been observed in coordinated glir in other complexes.[2] Superimposed on the seven-line spectrum is a broad absorption with a half-width of about 25 G. It is very probable that this absorption is due to Zn(glir)$_2$ which is formed according to eq 3.

$$2\text{Zn(glir)}^+ \rightleftarrows \text{Zn}^{2+} + \text{Zn(glir)}_2 \quad (3)$$

The analogous complex Mg(glir)$_2$ was isolated and was shown from frozen-solution spectra to have a triplet ground state.[1a] The triplet gives rise to one broad absorption in liquid solution. The resulting spectrum disappears rapidly (within a few minutes) after the electrolytic current is switched off. This radical species has a low stability compared with those complexes to be described later.

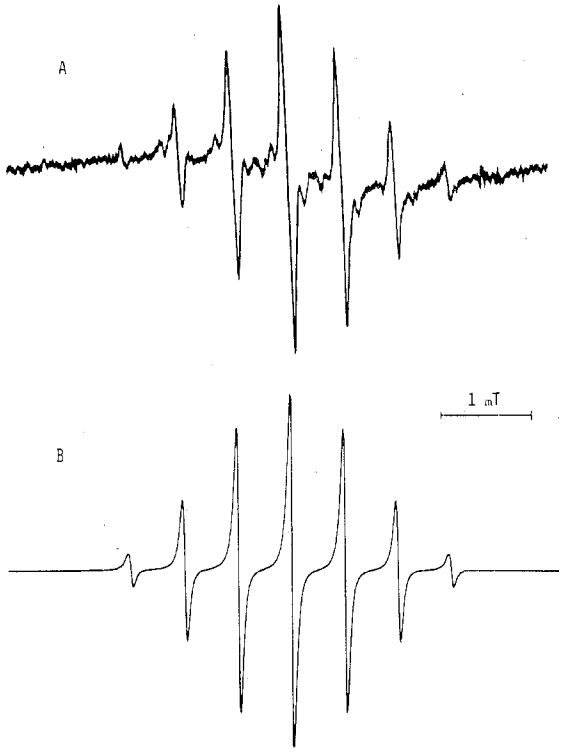

Figure 2. ESR spectrum of Zn(glir)$^+$: (A) experimental; (B) simulated. The broad absorption is probably due to Zn(glir)$_2$ and the weak narrow lines in (A) come from Zn(gli(r/2))$_2^+$ (Figure 5).

Addition of salts with coordinating anions or of neutral ligands in the titrand solution always results in a dramatic change in the ESR spectrum. With X^- = Cl$^-$, Br$^-$, NCS$^-$, NCO$^-$, and N$_3^-$, the species Zn(glir)X and Zn(glir)X$_2^-$ were identified by their ESR spectra. Addition of X^- to Zn(glir)$^+$ resulted in spectra which were superpositions of those of Zn(glir)$^+$ and Zn(glir)X until a certain amount of X^- was added. It was always possible to reach a concentration range where essentially only Zn(glir)X was present in detectable concentration. Upon further addition of X^- still another spectrum appeared consisting of the superposition of the spectra of Zn(glir)X and Zn(glir)X$_2^-$. In solutions with a high X^- concentration only Zn(glir)X$_2^-$ was observed. With I$^-$ only the 1:1 complex was obtained. Due to the low stability of the 1:1 complex, it could not be formed quantitatively.

The "pure" spectra, e.g., those of Zn(glir)$^+$, Zn(glir)X, and Zn(glir)X$_2^-$, were analyzed either by a visual best-fit procedure utilizing simulation of the spectra or by a least-squares fit procedure on spectra obtained in a digital form.[7] As examples the spectra of Zn(glir)N$_3$ and of Zn(glir)(N$_3$)$_2^-$ are shown in Figures 3 and 4. Small differences between measured and computed spectra are due to the presence of other radical species in small concentrations.

The coupling constants are given in Table I together with those of complexes to be described below. Relative concentrations in the intermediate concentration ranges with two paramagnetic species present were obtained by visual best-fit procedure with complete simulation of the superposed spectra.

Because the radical complexes were not completely stable under the experimental conditions (the signal decayed within some minutes after turning off the current), it was not attempted to measure absolute values of equilibrium constants. Some qualitative conclusions can be drawn however. The

Table I. Coupling Constants of Radical Complexes in DMF and DME[2] (All Values in mT)

Complex	a_H		a_H(DME)/ a_H(DMF)	a_N		a_N(DME)/ a_N(DMF)	a_X[b]		a_X(DME)/ a_X(DMF)	$a_X(1:1)/a_X(2:1)$	
	DMF	DME		DMF	DME		DMF	DME		DMF	DME
$Zn(glir)^+$	0.558			0.558							
Zn(glir)Cl	0.572	0.555	0.9703	0.572	0.555	0.9703	0.091	0.058	0.6374	0.5833	0.4143
$Zn(glir)Cl_2^-$ [a]	0.526	0.510	0.9696	0.607	0.572	0.9423	0.156	0.14	0.8974		
Zn(glir)Br	0.562	0.560	0.9964	0.562	0.560	0.9964	0.562	0.340	0.6050	0.6487	
$Zn(glir)Br_2^-$ [a]	0.627			0.559			0.886				
Zn(glir)NCO	0.564			0.564			0.064			0.5203	
$Zn(glir)(NCO)_2^-$ [a]	0.530			0.601			0.123				
Zn(glir)NCS	0.565			0.565			0.070			0.5426	
$Zn(glir)(NCS)_2^-$ [a]	0.559	0.533	0.9535	0.579	0.582	1.005	0.129	0.123	0.9535		
$Zn(glir)N_3$	0.565			0.565			0.06			0.6000	
$Zn(glir)(N_3)_2^-$ [a]	0.540			0.588			0.100				
Zn(glir)I	0.567			0.567			0.710				
$Zn(glir)en^+$	0.563			0.562			0.112				
$Zn(gli(r/2))_2^+$	0.305			0.305							

[a] Parameter values optimized using ESOP.[7] [b] Mean values are given for the two isotopes of Cl and Br.

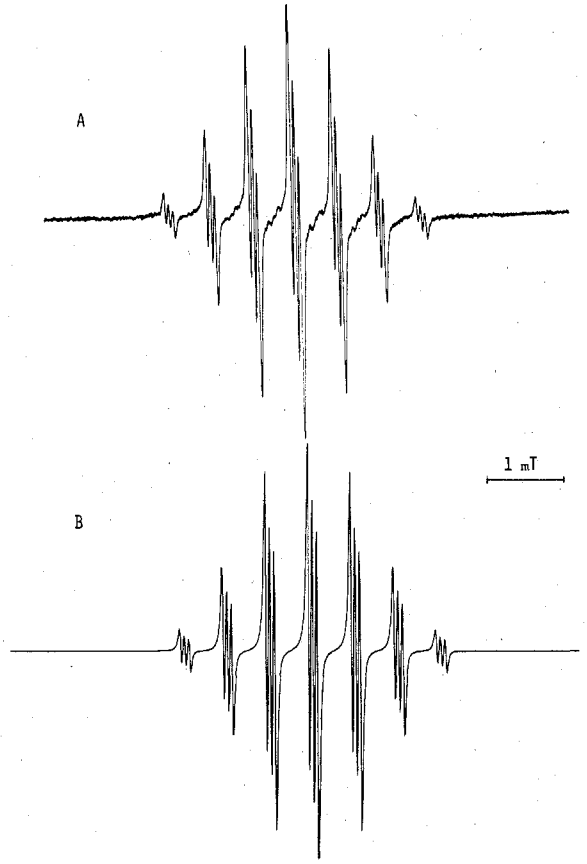

Figure 3. ESR spectrum of $Zn(glir)N_3$: (A) experimental; (B) simulated.

observability of "pure" Zn(glir)X over a rather broad concentration range can only be explained if $K_1 >> K_2$ in eq 4.

$$Zn(glir)^+ + X^- \overset{K_1}{\rightleftarrows} Zn(glir)X$$
$$Zn(glir)X + X^- \overset{K_2}{\rightleftarrows} Zn(glir)X_2^- \qquad (4)$$

A rough estimate from the concentration data yields $K_1/K_2 \approx 10^2$–10^3 which is far from the statistical value. This large ratio can be explained on electrostatic grounds and/or steric effects. The ligand glir is extremely bulky due to the two *tert*-butyl groups. The sequence of increasing stability, again roughly estimated from ESR intensities, is $I^- < NCO^- \sim Cl^- < Br^- < N_3^- < NCS^-$. In the case of I^-, the second step is dubious. After having reached Zn(glir)I, further addition of iodide yields a new complicated spectrum that has escaped interpretation so far.

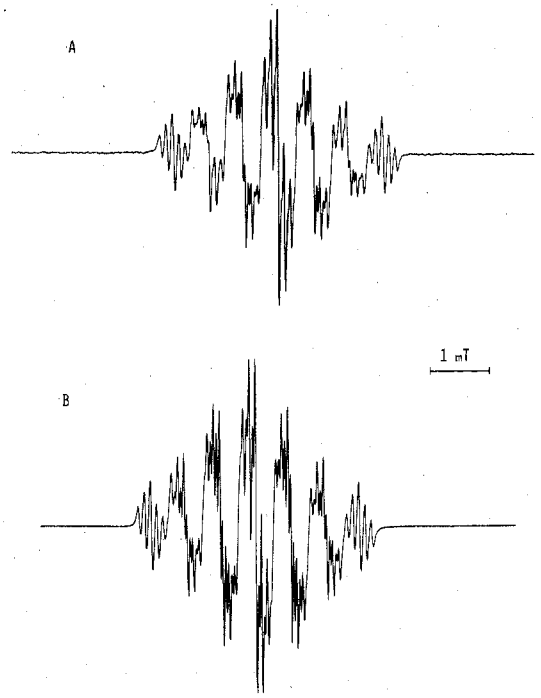

Figure 4. ESR spectrum of $Zn(glir)(N_3)_2^-$: (A) experimental; (B) simulated.

With uncharged monoamines (NH_3, CH_3NH_2, $(CH_3)_2NH$) no radical complexes could be observed. The chelate en gives in a one-step reaction a complex with the two nitrogen ligands forming an equivalent set.

A most interesting case is encountered if the ligand whose concentration is increased is gli. A second paramagnetic species besides $Zn(glir)^+$ can be observed in the ESR spectra with increasing gli concentration. Finally the spectrum of $Zn(glir)^+$ disappears and the one shown in Figure 5 can be observed. It is interpreted as being due to the interaction of the electron spin with four equivalent protons and four equivalent nitrogen nuclei with accidentally degenerate coupling constants of 3.05 G each. An excellent agreement is obtained between measured and simulated spectra with this assumption. The doubling of the number of equivalent nuclei and the reduction of the coupling constants by about a factor of 2 indicates a complete delocalization of the unpaired electron over the two orthogonal chelating ligands, at least on the ESR time scale, the two ligands being therefore in a collectively reduced state. In the nomenclature proposed for radical

complexes, this complex should be written as $Zn(gli(r/2))_2^+$, because each ligand gli carries formally half of the unpaired electron.

The rough concentration measurements indicate a stability for the coordination of gli which is about a factor 3 smaller than for en.

Discussion

Geometrical and Electronic Structure. Space-filling models of $Zn(glir)^+$ reveal a serious crowding of the *tert*-butyl groups in the neighborhood of the zinc ion. A coordination number exceeding 5 (trigonal bipyramid) seems to be excluded. For the complex $Zn(glir)X_2^-$, a tetrahedral coordination geometry seems to be most likely, although a five-coordinate structure with two axial X^- ligands cannot be completely excluded. Apart from the models, the coupling constants provide further evidence for a tetrahedral structure: contrary to the 1:1 complexes little variation of the coupling constants was found in those cases where the same species could be measured in the solvents DME and DMF (Table I). The near independence of the coupling constant from the medium makes a first-sphere coordination of solvent molecules unlikely. Almost certainly $Zn(glir)en^+$ is tetrahedrally coordinated, whereas Zn(glir)X and particularly $Zn(gli(r/2))_2^+$ deserve further consideration.

Since isolation of the complexes has been unsuccessful and is apt to be extremely difficult, if at all possible, some correlation between experimental data and the results of MO calculations was attempted. These calculations were based on the SCCC–MO model[8] using the method originally proposed by Wolfsberg and Helmholz.[9] A maximum number of 103 basis orbitals can be handled in the present version of the program. The following orbitals were considered: Zn, 3d, 4s, 4p; H, 1s; all other atoms, *n*s, *n*p. Radial functions were chosen according to Clementi.[10] For the off-diagonal elements the arithmetic mean method was chosen, with a proportionality factor of $K = 1.75$. For simplification the *tert*-butyl groups were replaced by hydrogen atoms.

For Zn(glir)X the following molecular geometries were considered: I, without solvent molecules in the first coordination sphere, *all* atoms of the molecule lying in one plane, a twofold axis going through Zn and X bisecting the C–C bond of glir; point group symmetry C_{2v}; II, two solvent molecules one below and one above the plane formed by Zn(glir)X, lying on an axis perpendicular to that plane; symmetry C_{2v} [because DMF would be too complicated to be considered in our calculations, the solvent molecules were taken as H_2O, since water has properties very similar to those of DMF as far as orbital energies in transition metals are concerned;[5] this molecule will be called $Zn(glir)X(S)_2$]; III, one solvent molecule completing a *tetrahedral* coordination sphere of Zn^{2+} [the symmetry of the molecule, called $Zn(glir)X(S)$, is C_s].

$Zn(glir)X_2$ was always taken in tetrahedral geometry (symmetry C_{2v}) with the triatomic groups $X = X_1–X_2–X_3$ (NCS^-, NCO^-, N_3^-) forming linear $Zn–X_1–X_2–X_3$ bonds. The SCCC condition was defined as being reached if no change in the charge of Zn was obtained in the fourth decimal place after one additional cycle in the calculation. The relevant data from the calculation are given in Table II.

The results from the calculations are qualitatively in good agreement with the experimental data. There is never an appreciable spin population outside the p_π (p_x) orbitals of glir, justifying the classification of such compounds as *radical complexes*. In view of the small variation no correlation is feasible between the spin populations in p_x^C and p_x^N and the corresponding coupling constants a_H and a_N. Q_{CH} obtained from a linear regression is 1.96 ± 0.08 mT.

If neighbor atom effects in the spin polarization on N are neglected, a proportionality constant of 2.77 ± 0.23 mT

Table II. SCCC–MO data of $Zn(glir)^+$, Zn(glir)X, Zn(glir)X(S), $Zn(glir)X(S)_2$, and $Zn(glir)X_2$ [a]

X (geometry I, II, or III[c])	Energies of semioccupied MO in eV	Self-consistent charge on Zn	Spin population											
			Zn		N	C	X_1		X_2[d]			X_3		
			d_{xz}	p_x	p_x	p_x	s	p_z	p_x	s	p_z	p_x	s	p_z	p_x
Cl^- (I)	−10.79	0.52	0.0005	0.0314	0.1897	0.2909			0.0071						
Cl^-H_2O (III)	−10.69	0.57	0.0012	0.0035	0.2150	0.2801	0.0002	0.0022	0.0010	0.0001	0.0008	0.0010			
$Cl^-(H_2O)_2$ (II)	−10.68	0.63	0.0004	0.0024	0.2195	0.2779			0.0003	0.0001	0.0000	0.0010			
$(Cl^-)_2$	−10.68	0.49	0.0013	0.0018	0.2177	0.2768	0.0002	0.0020	0.0018						
Br^- (I)	−10.78	0.48	0.0005	0.0281	0.1918	0.2882			0.0116						
$(Br^-)_2$	−10.68	0.43	0.0012	0.0012	0.2166	0.2749	0.0002	0.0038	0.0035						
N_3^- (I)	−10.82	0.55	0.0004	0.0445	0.1808	0.2930			0.0026			0.0016			0.0035
$(N_3^-)_2$	−10.69	0.56	0.0011	0.0034	0.2146	0.2797	0.0003	0.0004	0.0017	0.0000	0.0004	0.0000	0.0000	0.0008	0.0001
NCO^- (I)	−10.83	0.57	0.0004	0.0505	0.1774	0.2944			0.0004			0.0051			0.0004
$(NCO^-)_2$	−10.69	0.54	0.0011	0.0032	0.2154	0.2796	0.0004	0.0008	0.0013	0.0002	0.0002	0.0001	0.0000	0.0001	0.0002
NCS^- (I)	−10.81	0.56	0.0004	0.0418	0.1818	0.2917			0.0041			0.0005			0.0063
$(NCS^-)_2$	−10.70	0.54	0.0014	0.0051	0.2114	0.2794	0.0005	0.0033	0.0016	0.0002	0.0002	0.0001	0.0000	0.0003	0.0002
glir[b]	−10.92				0.2002	0.2998									

[a] Entries in the columns belonging to the different orbitals are spin populations. No entry means that there is either no atom or the spin population vanishes for symmetry reasons. The *x* axis is perpendicular to the Zn(glir) plane; *z* is bisecting the N–Zn–N angle. [b] Spin populations in uncoordinated glir were calculated using an extended Hückel procedure. [c] See text. [d] Oxygen orbitals in coordinated H_2O.

Table III. Spin Populations and Energies in the Highest Orbitals in the Complex Formed between $Zn(glir)^+$ and gli

Complex	Symmetry	Ligand a		Ligand b		Zn	Symmetry of the relevant orbital	Energy splitting of highest orbitals, eV
		C	N	C	N			
$Zn(gli(r/2))_2^+$	D_{2d}	0.1396	0.1093	0.1396	0.1093	0.0044	e	0
$Zn(gli(r/2))_2^+$	D_2, 45° between ligand planes	0.1424	0.1025	0.1424	0.1025	0.0190	b_2	0.105
$Zn(glir)(gli)^+$	C_{2v}	0.27605	0.2137	0.00005	0.077	0.0044	b_1	0.364

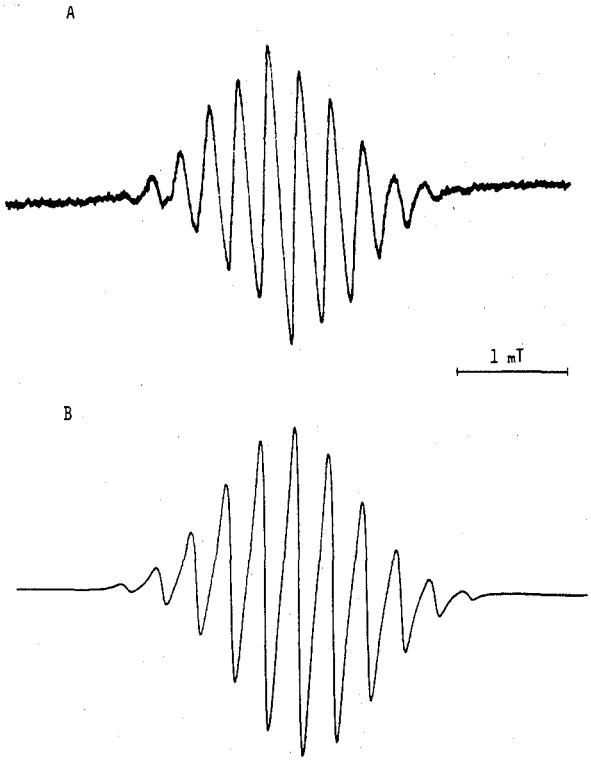

Figure 5. ESR spectrum of $Zn(gli(r/2))_2^+$: (A) experimental; (B) simulated.

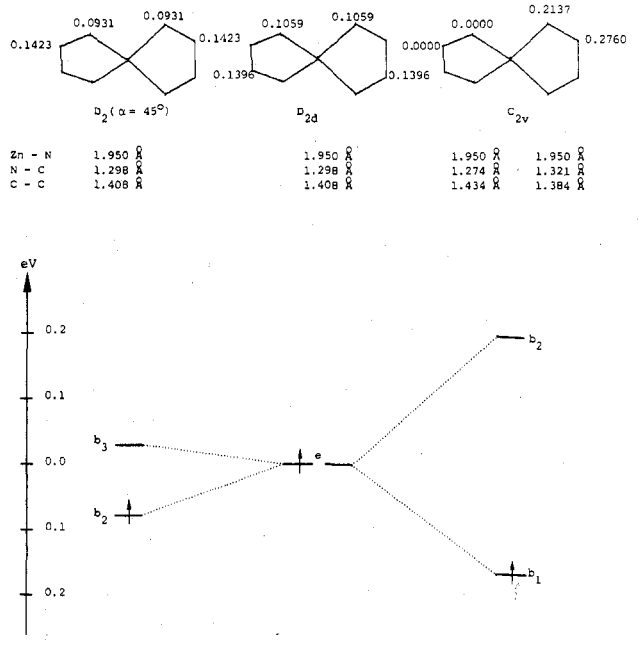

Figure 6. Correlation diagram for two distortions of the $Zn(gli(r/2))_2^+$ complex.

between spin population and the coupling constant a_N is obtained.

Coupling constants for Zn have not been measured with this method,[2] since large amounts of Zn are necessary and isotopic enrichment therefore was not feasible.

Coupling constants of X show one common property for all X, namely, that a_X is always significantly larger in $Zn(glir)X_2$ than in Zn(glir)X. The ratios are given in Table I for the various X groups together with the solvent dependence in those cases where measurements were made in DMF and DME. Spin density at the X nuclei in tetrahedral $Zn(glir)X_2$ complexes can result from spin polarization *and* direct spin delocalization into the s orbitals of X. In Zn(glir)X, however, a direct delocalization can be achieved only if it is tetrahedrally coordinated as in Zn(glir)X(S) (symmetry C_s), but not in Zn(glir)X (C_{2v}) nor in $Zn(glir)X(S)_2$ (C_{2v}). In the two latter cases, spin population in s orbitals is zero for symmetry reasons. We regard the experimental facts of strong solvent influence and the smaller value of a_X in Zn(glir)X as strong indications for $Zn(glir)X(S)_2$ species in solution. The order of magnitude of the increased a_X in $Zn(glir)X_2$ is correct if it is assumed that the spin polarization is equal in $Zn(glir)X_2$ and Zn(glir)X, and the difference $a_X^{Zn(glir)X_2} - a_X^{Zn(glir)X}$ is only caused by the s-orbital density. If one assumes, for example, the value of 1685 G for the isotropic coupling constant[11] of ^{35}Cl, a coupling constant of 0.34 G is obtained from the calculated spin density 0.0002. (The difference between the experimental coupling constants is 0.61 G.) The calculated s spin density on X is almost the same in Zn(glir)X(S) as in $Zn(glir)X_2$, and one would therefore expect similar coupling constants a_X for 1:1 and 2:1 complexes, for the tetrahedral structure.

$Zn(gli)_2^{2+}$ has point group symmetry D_{2d} if both ligands are assumed to be identical and perpendicular to each other. It has two degenerate lowest antibonding orbitals (LUMO) transforming as the irreducible representation e. This is the level that accommodates the unpaired electron in $Zn(gli(r/2))_2^+$ giving rise to a doubly degenerate ground state. The appropriate linear combination has been chosen in Table III where the spin densities in gli(r/2) are indeed about half as big as in the cases of coordinated glir. The symmetry of D_{2d} corresponds to a situation where a Jahn–Teller distortion would be expected. There are several possible distortions from D_{2d} which could lift the degeneracy of the ground state. Two of them were considered in detail: (a) a torsion of one chelate ring with respect to the other so that they are no longer perpendicular to each other (symmetry D_2); (b) a change in bond length in both ligands corresponding to the localization of the unpaired electron on one ligand. This complex could be formulated as $Zn(glir)(gli)^+$ and would have the symmetry C_{2v}.

For the calculations, average values were used for bond lengths in the ligands: $Zn(gli(r/2))_2^+$ (D_{2d} and D_2), C–C = 1.408 Å, C–N = 1.298 Å, Zn–N = 1.950 Å; $Zn(glir)(gli)^+$ (C_{2v}), C–C = 1.383 Å and C–N = 1.321 Å for glir and C–C = 1.434 Å and C–N = 1.274 Å for gli, Zn–N = 1.950 Å.

Values for the spin populations for the three cases are given in Table III.

A correlation diagram for the splitting of the e level is given in Figure 6. Considering just orbital energies, both kinds of distortions lead, of course, to a splitting of the e level of the D_{2d} case. Distortion to C_{2v} leads automatically to a nearly complete localization of the unpaired electron on one of the rings whereas distortion to D_2 symmetry leaves it delocalized (for the calculation only bond lengths have been changed). The distortion to C_{2v} is much more effective in lifting the degeneracy although an unrealistically large torsion angle of 45° has been assumed for the distortion to D_2. From these crude calculations one would therefore assume a double-minimum potential surface for the complex, where the minima correspond to states with the unpaired electron localized on one chelate ligand. The energy barrier is calculated to be about 0.17 eV. Such a value would lead, of course, to a rapid exchange of the unpaired electron from one ligand to the other, resulting in an apparent identity of the two ligands on the ESR time scale.

Acknowledgment. This work has been supported by the Swiss National Foundation for Scientific Research. We thank also Ciba-Geigy S.A., Basle, Switzerland, for financial support.

Registry No. $Zn(glir)^+$, 58002-31-6; $Zn(glir)Cl(DMF)_2$, 58002-32-7; $Zn(glir)Cl(DME)_2$, 58002-33-8; $Zn(glir)Cl_2^-$, 58002-34-9; $Zn(glir)Br(DMF)_2$, 58002-35-0; $Zn(glir)Br(DME)_2$, 58074-41-2; $Zn(glir)Br_2^-$, 58002-36-1; $Zn(glir)(NCO)(DMF)_2$, 58002-37-2; $Zn(glir)(NCO)_2^-$, 58002-38-3; $Zn(glir)(NCS)(DMF)_2$, 58002-39-4; $Zn(glir)(NCS)_2^-$, 36471-83-7; $Zn(glir)(N_3)(DMF)_2$, 58002-40-7; $Zn(glir)(N_3)_2^-$, 58002-41-8; $Zn(glir)I(DMF)_2$, 58002-42-9; $Zn(glir)en^+$, 58002-43-0; $Zn(gli(r/2))_2^+$, 58117-15-0; $Zn(glir)_2$, 58023-82-8.

Supplementary Material Available: Figures 7–16 showing the ESR spectra of the radical complexes generated electrolytically in DMF (10 pages). Ordering information is given on any current masthead page.

References and Notes

(1) (a) Part III: P. Clopath and A. v. Zelewsky, *Helv. Chim. Acta*, **56**, 980 (1973). (b) Abstracted in part from the Ph.D. Thesis of S. Richter, University of Fribourg, 1974.
(2) P. Clopath and A. v. Zelewsky, *Helv. Chim. Acta*, **55**, 52 (1972).
(3) It is proposed to add the letter r (radical) to the abbreviated name of a ligand which is present in the form of a radical, that is, a ligand carrying one unpaired electron. Charges are only given if necessary.
(4) C. T. Cazianis and D. R. Eaton, *Can. J. Chem.*, **52**, 2454 (1974).
(5) W. Schneider, *Helv. Chim. Acta*, **46**, 1842 (1963).
(6) O. Bravo and R. T. Iwamoto, *J. Electroanal. Chem.*, **23**, 419 (1969).
(7) Based on a program by J. P. Heinzer (Dissertation, Eidgenoessische Technische Hochschule, No. 4255, 1968) a new program ESOP was written in Fortran IV which operates also in the case where several isotopes of an element contribute to the hyperfine pattern, as in the halide complexes. This program is described in the Ph.D. thesis of C. Daul. It can be obtained from the authors upon request.
(8) We thank Mr. Seeger, Institut of Physical Chemistry, University of Basle, for the original form of the program.
(9) M. Wolfsberg and L. Helmholz, *J. Chem. Phys.*, **20**, 837 (1952).
(10) E. Clementi and D. L. Raimondi, *J. Chem. Phys.*, **38**, 2686 (1963).
(11) J. E. Wertz and J. R. Bolton, "Electron Spin Resonance: Elementary Theory and Practical Application", McGraw-Hill, New York, N.Y., 1972.

Contribution from the Department of Chemistry,
Sir George Williams Campus, Concordia University, Montreal, H3G-1M8, Canada

Configurational Rearrangements in *cis*-$M(AA)_2X_2$, *cis*-$M(AA)_2XY$, and *cis*-$M(AB)_2X_2$ Complexes. I. A Permutational Analysis[1]

DOUGLAS G. BICKLEY and NICK SERPONE*

Received June 19, 1975 AIC504382

A permutational analysis is described for the coalescence behavior of ^1H NMR probes in a nuclear magnetic resonance experiment, in which the probes are incorporated in bidentate (e.g., β-diketones, RCOCHR'COR") and/or monodentate (e.g., $-OCH(CH_3)_2$) ligands in stereochemically nonrigid complexes of the type *cis*-$M(AA)_2X_2$, *cis*-$M(AA)_2XY$, and *cis*-$M(AB)_2X_2$. Diastereotopic probes have been considered so as to follow the course of metal-centered configurational rearrangements. Changes in signal multiplicities resulting from averaging sets operating on the above complexes with or without diastereotopic ligands are discussed. Distinctions between averaging sets on the basis of changes in signal multiplicities are given. A correlation table of the various averaging sets derived for the three types of systems is presented, and it is proposed that once a unique averaging set has been determined for one of the above systems, this same averaging set can be correlated with those of another system for which a unique choice is not possible.

Introduction

Intramolecular exchange processes continue to confront inorganic and organometallic chemists with fascinating problems.[2] One particularly active area[3-6] deals with intramolecular rearrangement reactions of six-coordinate chelate complexes. Rearrangements may involve diastereomerization and/or enantiomerization, and a classification of metal chelates in terms of their rearrangement rates has introduced the designations "slow" and "fast".[7] Stereochemically nonrigid or fast complexes exhibit rearrangement rates that are too large to permit isolation of diastereomers and enantiomers but do allow isomer detection and, in some cases, kinetic studies by nuclear magnetic resonance (NMR) line shape analysis.

It is now well recognized[8] that when a $-CXY_2$ group is bound to some dissymmetric group, the two Y substituents neither achieve equivalence in any rotational conformation nor achieve it as a result of internal rotation, however rapid. To achieve equivalence, inversion of the dissymmetric moiety must occur. Incorporation of a diastereotopic group within the chelate ring may thus enable enantiomerization processes to be detected and rates to be measured. This ability to detect enantiomerization processes in nonrigid chelates has enabled significant progress in the elucidation of the mechanism(s) of rearrangement. Physical rearrangement pathways are generally considered to be of two limiting types:[3,4] (i) twist motions proceeding about axes passing through octahedral faces via an idealized trigonal-prismatic transition state and (ii) bond rupture processes via a five-coordinate trigonal-bipyramidal or square-pyramidal transition state, with, in each case, dangling axial or equatorial (basal) ligands. While these two distinct types of mechanisms are physically reasonable, there is no assurance that every feasible mechanism has been considered.

An inherent problem[6,9] often faced in dynamic NMR studies is that the NMR experiment does not define the actual configurational changes during the rearrangement but rather defines a particular site interchange pattern. In order to overcome this problem and also to ensure that every feasible mechanism has been considered, permutational analyses have recently been applied[10-24] to six-coordinate molecules to